NANO LETTERS

Letter

pubs.acs.org/NanoLett

Optically Active Metasurface with Non-Chiral Plasmonic Nanoantennas

Amr Shaltout, Jingjing Liu, Vladimir M. Shalaev, and Alexander V. Kildishev*

Birck Nanotechnology Center, School of Electrical and Computer Engineering, Purdue University, West Lafayette, Indiana 47907, United States

Supporting Information

ABSTRACT: We design, fabricate, and experimentally demonstrate an optically active metasurface of $\lambda/50$ thickness that rotates linearly polarized light by 45° over a broadband wavelength range in the near IR region. The rotation is achieved through the use of a planar array of plasmonic nanoantennas, which generates a fixed phase-shift between the left circular polarized and right circular polarized components of the incident light. Our approach is built on a new supercell metasurface design methodology: by judiciously designing the location and orientation of individual antennas in the structural supercells, we achieve *an effective chiral metasurface* through *a collective operation of nonchiral antennas*. This approach simplifies the overall structure when compared to designs with chiral antennas and also enables a chiral effect which *quantitatively* depends solely on the supercell geometry. This allows for greater tolerance against fabrication and temperature effects.

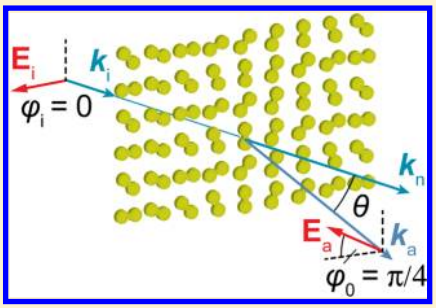

KEYWORDS: *metasurfaces, optical activity, plasmonic antennas*

An optically active material produces a different response to right circularly polarized (RCP) and left circularly polarized (LCP) light,[1] thereby rotating the angle of linearly polarized light along the propagating direction. The importance of optical activity transcends optical applications and is of immense value to sensing applications in stereochemistry,[2] molecular biology,[3] crystallography,[4] and secure quantum communications.[5] It is typically obtained using chiral structures, which do not superimpose onto their mirror image, lifting the degeneracy of LCP and RCP. The effect is generally weak in natural materials and detectable only when strong phase differences between LCP and RCP accumulate over a long optical path. With the advent of nanotechnology, strong optical activity using artificially structured materials have been demonstrated. To achieve the rotation of the electromagnetic field vectors, structures are designed to rotate with angular offset along the propagation direction and possess directional mirror asymmetry. Design and fabrication of such chiral structures[6−13] is complicated because they require multiple fabrication steps to complete the angular rotations assigned for successive layers in a third dimension. Complexity can be reduced using optical metasurfaces,[14] which are metamaterials with reduced dimensionality[15] and typically consist of a 2D array of plasmonic antennas. Such metasurfaces can alter the phase or polarization of incident light abruptly, enabling effects identical to naturally birefringent and chiral media. They have been successfully used in many applications including light bending,[14,16] flat lenses,[17−19] circular polarizers,[20] half-wave plates[21,22] and quarter-wave plates.[23−25] Metasurfaces have also been used to obtain optical activity (OA) using planar chiral structures,[26−30] where optical activity was obtained either through intrinsic or extrinsic chirality of antennas. Intrinsic chiral antennas do not superimpose onto their mirror image, whereas extrinsic antennas only break mirror symmetry under oblique incidence and cannot obtain chiral properties if light is normally incident. For both cases, there has been no clear strategy to design a metasurface with a specific OA angle.

In this work, a desired OA is obtained using an optical metasurface with a different approach other than the intrinsic or extrinsic chirality of nanoantennas. Here, we present an array of nanoantennas, which individually are nonchiral but where chirality is obtained through the collective contribution of the entire array or, more specifically, through the array of supercells. This avoids both the complex structure of intrinsic chiral antennas and the incident angle dependence of extrinsic chiral antennas. Additionally, a design methodology is introduced to realize a rotation of polarization angle (PA) to any specific value (45° in our case), accurately determined by the geometry of structure rather than the intrinsic properties of composite materials. In previous 2D and 3D chiral structures, there was no quantitative formula between the introduced chiral effect and the geometry of the structure. The typical procedure was to design an asymmetric structure with a handedness that relates qualitatively to the required chiral effect and then to optimize it quantitatively through simulation and experimentation. Having a quantitative formula relating the chiral effect to the structure's geometry facilitates the designer's work and secures stability against fabrication and temperature

Received: April 15, 2014
Revised: July 19, 2014
Published: July 22, 2014

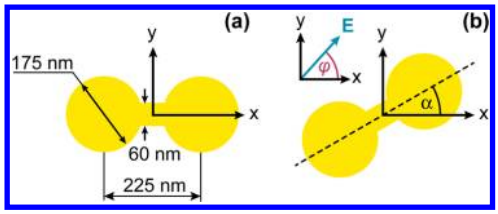

Figure 1. Top-view schematic geometry of a single nanoantenna. (a) Designed dimensions of an elemental 30 nm thick nanoantentenna; (b) nanoantenna tilted at angle α with respect to x axis. Inset: PA φ between the E-field and the horizontal (x) axis. Light propagates perpendicular to the xy-plane (out of the figure plane).

effects. Our goal is achieved through splitting the circular components of the incident beam and introducing an optical phase delay between the opposite polarizations.[24] The rotation of PA is related to the introduced phase difference as will be explained below,[1] and based on this relation, it will be shown how our metasurface is designed to achieve its determined functionality.

A linearly polarized (LP) light with an angle of polarization φ as shown in inset of Figure 1 can be written as a superposition of its circular components as follows:

$$\mathbf{E} = E_0(\hat{\mathbf{x}}\cos\varphi + \hat{\mathbf{y}}\sin\varphi) = \frac{E_0}{\sqrt{2}}(\hat{\mathbf{r}}e^{-i\varphi} + \hat{\mathbf{l}}e^{i\varphi}) \quad (1)$$

where $\hat{\mathbf{r}} = (\hat{\mathbf{x}} + i\hat{\mathbf{y}})/\sqrt{2}$ and $\hat{\mathbf{l}} = (\hat{\mathbf{x}} - i\hat{\mathbf{y}})/\sqrt{2}$ are the unit vectors of the RCP and LCP respectively. Equation 1 indicates that a phase delay of 2φ introduced to the RCP component with respect to the LCP component will cause a rotation of PA by a value of φ, and the PA will reverse from φ to $-\varphi$, if the RCP and the LCP coefficients are switched.

Hence, the role of the proposed metasurface is to introduce a required phase shift between the LCP and RCP components. Our approach is to split the circular components, and then introduce optical path delay between them to obtain the required phase shift. To split the LCP and the RCP, we use the metasurface design shown in Figure 2 which is made of an antenna array with a period of eight antennas (shown in Figure 1) such that any two adjacent antennas have a difference in α of 22.5°. The individual antennas are separated by 500 nm; hence, forming a periodic supercell with a lattice constant (p) of 4 μm. It has been demonstrated[31] that such a metasurface, upon excitation with circularly polarized light, transmits two beams. A circular copolarized beam is normally transmitted, while another cross-circular-polarized component is deflected in an anomalous direction by an angle $\theta = \sin^{-1}(\lambda/p)$ (direction of the first-order diffraction). A more detailed explanation of this effect is in the Supporting Information. It has also been shown[31] that the cross-circular-polarized term is deflected in the opposite direction when the incident beam is reversed from LCP to RCP, as shown in Figure 2a. Figure 2b shows the effect of exciting the metasurface with a linearly polarized light. By superposition of the cases in Figure 2a, the normal beams will add up to the same polarization state as the input, and the anomalous portion of the linearly polarized input beam is split into its circular components in two opposite diffraction directions. This is a very simple circular beam splitting structure supporting background-free circular components in two distinct diffraction directions.

The optical effect that is implemented in this work is the optical rotation of linearly polarized light, and to obtain it, we must take the structure described in Figure 2 one step further. To retrieve linearly polarized light in the output in the anomalous direction, we use two subarrays of anisotropic nanoantennas rotating in opposite directions as shown in Figure 3 (two subarrays in blue and red). This will cause the RCP from one subarray to be directed parallel to the LCP obtained from the other one, and the two rays effectively retrieve a linearly polarized output ray. The two output rays are deflected at opposite angles of $\theta = \sin^{-1}(\lambda/p)$. An offset distance $d = p/4$ is introduced between the two subunits to cause a $\pi/2$ phase shift between RCP and LCP, leading to a 45° rotation of the output angle of polarization according to eq 1. The value of the phase shift is $\pi/2$ because for the first order diffraction, the phase shift varies linearly with offset distance taking the value of $2\pi d/p$. The technique of using the offset distance to obtain a phase shift has been used before in different application to form a quarter wave plate.[24] The rotation of the PA is related then to the geometry by the formula

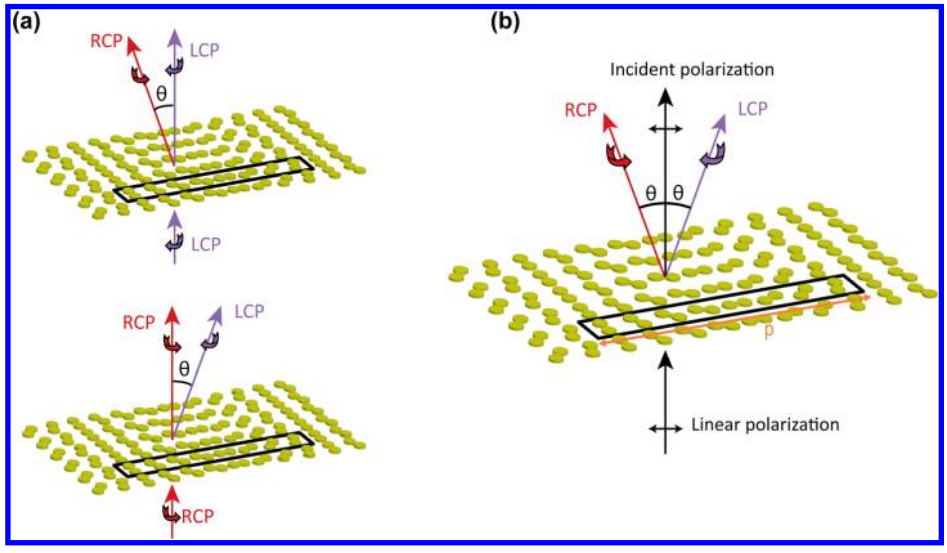

Figure 2. Metasurface structure for circular beam splitting: (a) effect of the metasurface on circularly polarized incident light and (b) applying superposition to obtain circular beam splitting effect for linearly polarized incident light; a part of the beam is transmitted normally with no change.

dx.doi.org/10.1021/nl501396d | Nano Lett. 2014, 14, 4426−4431

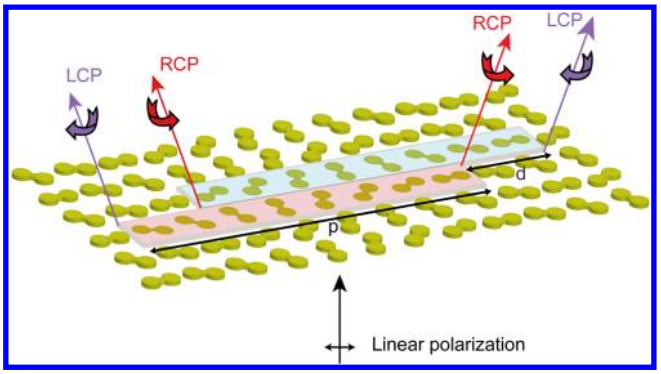

Figure 3. Metasurface structure that performs optical rotation. It consists of two subarrays (in blue and red) causing circular polarization splitting in two opposite diffraction directions. In each diffraction direction, LCP and RCP add up to retrieve linear polarization. The two subarrays are separated by an offset distance p, causing a phase shift between the LCP and the RCP, which results in rotation of angle of polarization for the linearly polarized output light.

$$\text{rotation angle} = 180^0 \times \frac{d}{p} \tag{2}$$

Equation 2 guarantees that the optical effect can be accurately determined by the designer and is immune against effects that could deteriorate the operation like changes to material properties due to temperature or fabrication.

This concludes that we obtain a normally transmitted beam with unchanged state of polarization and other two anomalously transmitted beams deflected in opposite directions with the required state of rotation of PA by 45°. Figure 4a demonstrates the overall performance of the metasurface subject to linearly polarized incident light.

Standard electron-beam lithography and lift-off processes are used to fabricate the array of gold nanoantennas on top of indium−tin-oxide coated glass substrate. Figure 4b is a field emission scanning electron microscope (FE SEM) image of the sample (a top view image taken from the gold nanoantenna side). Details of fabrication process are discussed in Supporting Information.

The operation of the metasurface is first tested in the transmission direction as shown in Figure 5a. The incident ray is shown in black, the normally transmitted ray in blue, and the anomalously transmitted ray in red. The anomalous transmission is the ray of interest and it occurs at some deflection angle θ_t. The experimental setup contains a tunable monochromatic source providing signal in the near IR regime, a polarizer to control the PA of the incident light (φ_i), and a rotating analyzer which filters the output power at different PA's (φ_0) to determine its polarization state. More details about experimental setup are shown in Supporting Information. Measurements are taken using an ellipsometer device which allows rotation of detector to detect the anomalous ray as a function of deflection angle θ_t. The output and input PA's of this structure are related by the formula

$$\varphi_0 = 45^0 - \varphi_i \tag{3}$$

The negative sign in eq 3 is coming from the switching from RCP to LCP and vice versa in anomalous transmission with respect to incident beam as shown in Figure 2a, and this results in changing the sign of φ as discussed after eq 1. To test the rotation of the PA, we checked it with four specific values of incident PA which are φ_i = 0, 45°, 90°, 135° (−45°). This is because these particular set of PA's uniquely defines any state of linear polarization from Stokes' parameters. Figure 5b and c show a sample of the results at φ_i = 0, 45° and the total set of results are presented in the Supporting Information.

These measurements are taken at λ = 1.5 μm and the anomalous output beam intensity is plotted as a function of the scattering angle θ_t. The validity of eq 3 is verified by measuring the output without polarization filtering, and then filtering the output at two different PA's (φ_0), which are the polarization directions defined by eq 3 and the orthogonal direction. The results show that the power at the expected value of φ_0 coincides with the total power, and the power in orthogonal direction is almost zero verifying the required operation. The ratio between the power in the desired and orthogonal directions is about 20 dB.

The operation of the metasurface is then tested in the reflection direction as shown in Figure 6a and d. We need two sets of measurements from both the nanoantennas side and the glass side because the handedness of the antenna array in Figure 3 is going to be flipped causing rotation of PA in opposite directions.

Since the reflected and transmitted circular components of light are of opposite polarizations, φ_0 of the anomalous reflected light incident from the nanoantenna side will be opposite to the one of the anomalous transmitted light in eq 3 and is given by

$$\varphi_0 = \varphi_i - 45^0 \tag{4}$$

Hence, for the anomalous reflection from glass side, different handedness of the array will cause φ_0 to obey the formula

$$\varphi_0 = \varphi_i + 45^0 \tag{5}$$

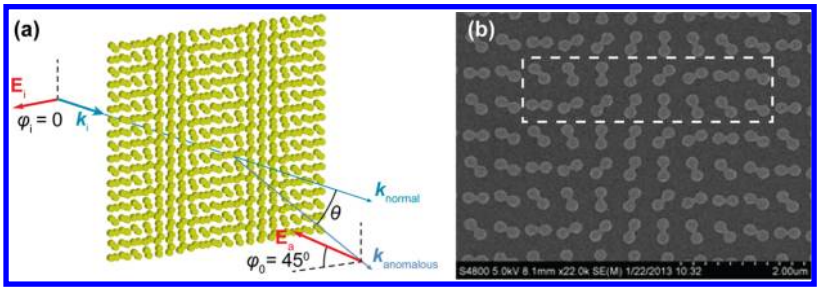

Figure 4. (a) The overall action of metasurface structure that performs optical rotation. There is a normal output beam with the same polarization as the input, and one of two anomalous output beams of interest deflected by an angle θ and optical rotation occurs to that beam by an angle 45°. (b) FE SEM top image of the fabricated sample with dashed rectangle to demonstrate the supercell.

dx.doi.org/10.1021/nl501396d | Nano Lett. 2014, 14, 4426−4431

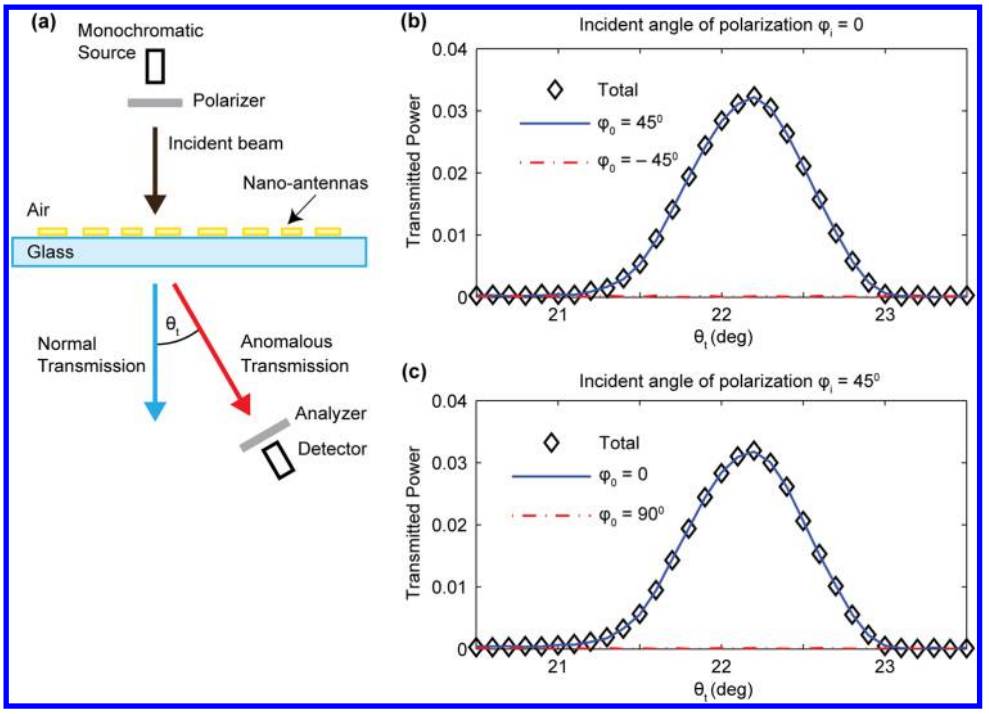

Figure 5. (a) Schematics of the experimental setup for testing the metasurface in the transmission mode. (b) Experimental results for incident PA $\varphi_i = 0$ showing that output power is at $\varphi_0 = 45°$. (c) Experimental results for incident PA $\varphi_i = 45°$ showing that output power is at $\varphi_0 = 0$.

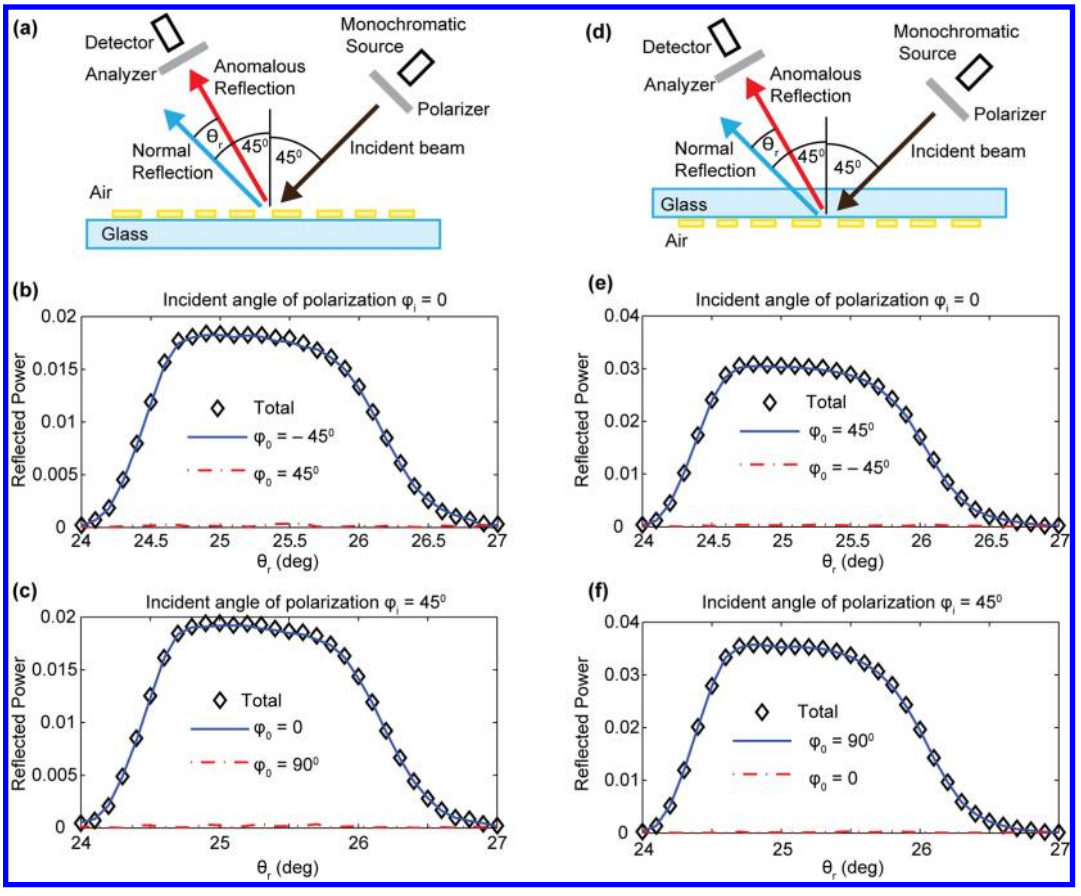

Figure 6. (a–c) Experimental setup and results for testing the metasurface in the reflection mode from the nanoantenna side. For $\varphi_i = 0$, the output power is at $\varphi_0 = -45°$, and for $\varphi_i = 45°$, the output power is at $\varphi_0 = 0$. (d–f) The setup and observed results in the reflection mode from the glass side. For $\varphi_i = 0$, the output power is at $\varphi_0 = 45°$, and for $\varphi_i = 45°$, the output power is at $\varphi_0 = 90°$.

dx.doi.org/10.1021/nl501396d | *Nano Lett.* 2014, 14, 4426–4431

For the transmission case, it will be redundant to show results for light incident from both sides of metasurface owing to the reciprocity of transmission operation. Figure 6 shows the validity of eqs 4 and 5 at $\lambda = 1.5$ μm for $\varphi_i = 0, 45°$; additional results are found in the Supporting Information. The output power in the desired anomalous beam was about 4%. It has been successfully demonstrated, though, that by utilizing metasurfaces in reflection mode,[32−34] their output could be enhanced by an order of magnitude, and such designs are also applicable in our case.

To analyze how broadband is the effect, we test it for the case of transmission from nanoantennas side with the input angle of polarization $\varphi_i = 0$, which is the same case as in Figure 5, but it is done for a set of wavelengths ranging from 1.05 to 1.7 μm. Outside this wavelength range, the performance deviates from the required functionality. Figure 7 shows the results for different wavelength values.

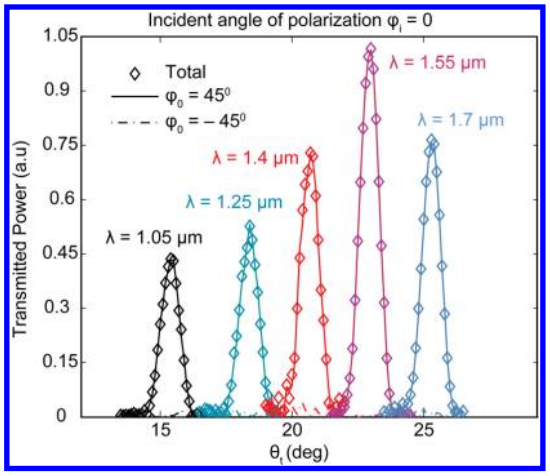

Figure 7. Experimental results for transmitted power at different wavelengths, with normally incident light for incident PA $\varphi_i = 0°$. The output power is at $\varphi_0 = 45°$ similar to Figure 5b for a broadband wavelength range from 1.05 to 1.7 μm. For each wavelength, the peak intensity occurs at a diffraction angle of $\theta = \sin^{-1}(\lambda/p)$.

In conclusion, a broadband chirality effect using ultrathin metasurface has been demonstrated. The structure is simple because it does not utilize complicated chiral meta-atoms, but rather chirality is obtained through the specific arrangement of nonchiral elements in periodic supercells. A methodology of metasurface supercell design to manipulate helical components of light is presented, which enables quantitative description of chiral effects as a function of geometrical dimensions of the structure. Dependence on the supercell geometry rather than the intrinsic properties of the individual antennas provides functional immunity against fabrication and temperature effects. There is a possibility to obtain tunable chiral effects in the future using the presented approach by incorporating micro-electromechanical systems (MEMS) technology to allow control of the geometrical distances responsible for the effective chirality of metasurface.

■ ASSOCIATED CONTENT

Supporting Information

Theoretical explanation of the structure; materials, fabrication, and optical characteristics; and experimental results for the whole set of incident polarization angles. This material is available free of charge via the Internet at http://pubs.acs.org.

■ AUTHOR INFORMATION

Corresponding Author

*E-mail: kildishev@purdue.edu.

Notes

The authors declare no competing financial interest.

■ ACKNOWLEDGMENTS

This work was partially supported by AFOSR grant FA9550-10-1-0264, ARO grant 63133-PH (W911NF-13-1-0226), and MRSEC NSF grant DMR-1120923.

■ REFERENCES

(1) Barron, L. D. *Molecular light scattering and optical activity*; Cambridge University Press: New York, 2004.
(2) Green, M. M.; Andreola, C.; Munoz, B.; Reidy, M. P.; Zero, K. *J. Am. Chem. Soc.* **1988**, *110*, 4063−4065.
(3) Fasman, G. D. *Handbook of Biochemistry and Molecular Biology: Physical and Chemical Data*. CRC press: Boca Raton, FL, 1976; Vol. 2.
(4) Glazer, A.; Stadnicka, K. *J. Appl. Crystallogr.* **1986**, *19*, 108−122.
(5) Bennett, C. H.; Brassard, G. *Proc. IEEE Int. Conf. Comput., Syst. Signal Process.* **1984**, 175−179.
(6) Gansel, J. K.; Thiel, M.; Rill, M. S.; Decker, M.; Bade, K.; Saile, V.; Von Freymann, G.; Linden, S.; Wegener, M. *Science* **2009**, *325*, 1513−1515.
(7) Zhang, S.; Park, Y.-S.; Li, J.; Lu, X.; Zhang, W.; Zhang, X. *Phys. Rev. Lett.* **2009**, *102*, 023901.
(8) Kwon, D.-H.; Werner, D. H.; Kildishev, A. V.; Shalaev, V. M. *Opt. Express* **2008**, *16*, 11822−11829.
(9) Plum, E.; Zhou, J.; Dong, J.; Fedotov, V.; Koschny, T.; Soukoulis, C.; Zheludev, N. *Phys. Rev. B* **2009**, *79*, 035407.
(10) Decker, M.; Klein, M.; Wegener, M.; Linden, S. *Opt. Lett.* **2007**, *32*, 856−858.
(11) Wang, B.; Zhou, J.; Koschny, T.; Soukoulis, C. M. *Appl. Phys. Lett.* **2009**, *94*, 151112.
(12) Li, T.; Liu, H.; Li, T.; Wang, S.; Wang, F.; Wu, R.; Chen, P.; Zhu, S.; Zhang, X. *Appl. Phys. Lett.* **2008**, *92*, 131111.
(13) Zhang, S.; Zhou, J.; Park, Y.-S.; Rho, J.; Singh, R.; Nam, S.; Azad, A. K.; Chen, H.-T.; Yin, X.; Taylor, A. J. *Nat. Commun.* **2012**, *3*, 942.
(14) Yu, N.; Genevet, P.; Kats, M. A.; Aieta, F.; Tetienne, J. P.; Capasso, F.; Gaburro, Z. *Science* **2011**, *334*, 333−337.
(15) Kildishev, A. V.; Boltasseva, A.; Shalaev, V. M. *Science* **2013**, *339*, 1232009.
(16) Ni, X.; Emani, N. K.; Kildishev, A. V.; Boltasseva, A.; Shalaev, V. M. *Science* **2012**, *335*, 427−427.
(17) Aieta, F.; Genevet, P.; Kats, M. A.; Yu, N.; Blanchard, R.; Gaburro, Z.; Capasso, F. *Nano Lett.* **2012**, *12*, 4932−4936.
(18) Ni, X.; Ishii, S.; Kildishev, A. V.; Shalaev, V. M. *Light: Sci. Appl.* **2013**, *2*, e72.
(19) Chen, X.; Huang, L.; Mühlenbernd, H.; Li, G.; Bai, B.; Tan, Q.; Jin, G.; Qiu, C.-W.; Zhang, S.; Zentgraf, T. *Nat. Commun.* **2012**, *3*, 1198.
(20) Zhao, Y.; Belkin, M.; Alù, A. *Nat. Commun.* **2012**, *3*, 870.
(21) Hao, J.; Yuan, Y.; Ran, L.; Jiang, T.; Kong, J. A.; Chan, C.; Zhou, L. *Phys. Rev. Lett.* **2007**, *99*, 063908.
(22) Zhu, Z.; Guo, C.; Liu, K.; Ye, W.; Yuan, X.; Yang, B.; Ma, T. *Opt. Lett.* **2012**, *37*, 698−700.
(23) Pors, A.; Nielsen, M. G.; Valle, G. D.; Willatzen, M.; Albrektsen, O.; Bozhevolnyi, S. I. *Opt. Lett.* **2011**, *36*, 1626−1628.
(24) Yu, N.; Aieta, F.; Genevet, P.; Kats, M. A.; Gaburro, Z.; Capasso, F. *Nano Lett.* **2012**, *12*, 6328−6333.
(25) Zhao, Y.; Alù, A. *Nano Lett.* **2013**, *13*, 1086−1091.
(26) Svirko, Y.; Zheludev, N.; Osipov, M. *Appl. Phys. Lett.* **2001**, *78*, 498−500.
(27) Prosvirnin, S. L.; Zheludev, N. I. *Journal Opt. A: Pure Appl. Opt.* **2009**, *11*, 074002.

(28) Plum, E.; Liu, X.-X.; Fedotov, V.; Chen, Y.; Tsai, D.; Zheludev, N. *Phys. Rev. Lett.* **2009**, *102*, 113902.
(29) Prosvirnin, S.; Zheludev, N. *Phys. Rev. E* **2005**, *71*, 037603.
(30) Papakostas, A.; Potts, A.; Bagnall, D.; Prosvirnin, S.; Coles, H.; Zheludev, N. *Phys. Rev. Lett.* **2003**, *90*, 107404.
(31) Kang, M.; Feng, T.; Wang, H.-T.; Li, J. *Opt. Express* **2012**, *20*, 15882−15890.
(32) Sun, S.; Yang, K.-Y.; Wang, C.-M.; Juan, T.-K.; Chen, W. T.; Liao, C. Y.; He, Q.; Xiao, S.; Kung, W.-T.; Guo, G.-Y. *Nano Lett.* **2012**, *12*, 6223−6229.
(33) Pors, A.; Nielsen, M. G.; Eriksen, R. L.; Bozhevolnyi, S. I. *Nano Lett.* **2013**, *13*, 829−834.
(34) Pors, A.; Albrektsen, O.; Radko, I. P.; Bozhevolnyi, S. I. *Sci. Rep.* **2013**, *3*, 2155.